

New Simulations for COIL lasers from the University of Illinois

D. S. Stromberg, L. A. Fockler, D. L. Carroll, and W. C. Solomon
University of Illinois at Urbana-Champaign

Abstract

Over the past six years we have been conducting detailed studies of a family of closely related supersonic mixing nozzles. These nozzles have performed well in experiments with the VertiCOIL laser. Subtle design changes in these nozzles lead to highly predictable results when compared to the complete CFD calculations for the three designs under study. Our conclusion is that mixing within the jets very near the nozzle throat with nitrogen diluent provides a more efficient lasing process.

Introduction and Background

The first supersonic COIL device was demonstrated in 1987 and reported by the Air Force Research Laboratory in 1988¹ and technology developments were reviewed in a 1992 paper.² A number of earlier computational studies have established the basic modeling approach. Pioneering work with detailed models was performed by Buggeln,³ and Madden,⁴ and Masuda⁵. These researchers and ourselves have taken similar approaches to coupling the COIL finite-rate kinetics with a detailed species molecular diffusion model. Research by Madden,⁴ Fockler,⁶ and Stromberg⁷ using the 3-D Navier-Stokes GASP code modeled enough detail to exactly represent the chemically reacting flowfield of the COIL under non-lasing conditions. This allows one to first determine the nature of the fundamental mixing and reacting flow before coupling the radiation transport to the simulation. Over the series of comparisons with existing VertiCOIL hardware^{8,9} we have established the viability and accuracy of the existing model. We recently applied the general simulation methodology to evaluating new COIL hardware configurations.

Over the past six years we have conducted detailed studies of the flow-fields within COIL lasers. We have chosen to study a family of closely related supersonic mixing nozzles that have performed well in experiments with the VertiCOIL laser. All designs have been tested experimentally to give substance to the computational results. In the present case we compare the operation of the VertiCOIL laser in our laboratory to the computational result for the mixing and reacting flow device operating with nitrogen diluent. In an earlier simulation⁶ a detailed CFD study of this laser in which helium was used as the diluent was conducted.

The Numerical Experiment

A schematic representation of a typical COIL is shown in Fig. 1. Our numerical experiment is designed to match VertiCOIL geometry and flow rates. The singlet-delta oxygen generator in our case is of the rotating disk type. The oxygen generator is close-coupled to the subsonic mixing chamber and molecular Iodine is introduced with a variety of sonic jets into the subsonic portion of the flow. The mixing and reacting flow is expanded through a Mach 2 supersonic nozzle into the laser cavity. The flow is subsequently discharged into a vacuum exhaust scrubber arrangement. Table 1 shows the rate constants of the important 13-reaction rate set within the COIL laser.

The chemical reaction set selected for this study is an updated 13-reaction set originally suggested by Carroll¹⁰ and later modified by Carroll¹¹ to include the new rates for Iodine deactivation measured by Heaven.¹² Our rationale for using this reduced reaction set in the studies covered here is given by Carroll.¹⁰ A close-up view of the important secondary injection-throat region of the nozzle is found in Figure 2. As can be seen we use a tight grid distribution within the sonic injectors and around the important injection region.

The flowfield within the VertiCOIL mixing nozzle is a low Reynolds number, viscous, chemically reacting flow with complex inviscid-viscid flow interactions. The flow is predominantly laminar, and viscous effects dominate a substantial portion of the flowfield. The second aspect consists of the core flow of the underexpanded jet which expands rapidly to form shocks as it decelerates. The third aspect is the transonic flow which produces strong streamwise gradients as the entire flow accelerates

though the nozzle. The Navier-Stokes fluid equations are appropriate to treat this chemically reacting flow, with its strong viscous-inviscid interactions.

Table 1. Reduced oxygen-iodine reaction set; 13 reactions, 10 species [I, I*, I₂, I₂*, N₂, H₂O, O₂(¹Δ), O₂(³Σ), O₂(¹Σ), Cl₂], Refs. 10-12.

<i>k</i>							Rates, cc/molecule-s	
<i>I₂ Dissociation</i>								
1	O ₂ (¹ Δ)	+	O ₂ (¹ Δ)	→	O ₂ (¹ Σ)	+	O ₂ (³ Σ)	2.5e-17
2	I ₂	+	O ₂ (¹ Σ)	→	2I	+	O ₂ (³ Σ)	4.0e-12
3	I ₂	+	O ₂ (¹ Δ)	→	I ₂ *	+	O ₂ (³ Σ)	7.0e-15
4	I ₂ *	+	O ₂ (¹ Δ)	→	2I	+	O ₂ (³ Σ)	3.0e-10
<i>I* Production</i>								
5	I	+	O ₂ (¹ Δ)	→	I*	+	O ₂ (³ Σ)	7.8e-11
6	I*	+	O ₂ (³ Σ)	→	I	+	O ₂ (¹ Δ)	1.04e-10*exp(-401.4/T)
7	I ₂	+	I*	→	I	+	I ₂ *	3.5e-11
8	I*	+	O ₂ (¹ Δ)	→	I	+	O ₂ (¹ Σ)	1.0e-13
<i>Deactivation Losses</i>								
9	I ₂ *	+	O ₂ (³ Σ)	→	I ₂	+	O ₂ (³ Σ)	4.9e-12
10	O ₂ (¹ Σ)	+	H ₂ O	→	O ₂ (³ Σ)	+	H ₂ O	6.7e-12
11	I ₂ *	+	H ₂ O	→	I ₂	+	H ₂ O	1.7e-11
12	I ₂ *	+	N ₂	→	I ₂	+	N ₂	8.2e-12
13	I*	+	H ₂ O	→	I	+	H ₂ O	2.1e-12

We employ a parallel version of the CFD code GASP to perform all the simulations reported in this investigation.^{13, 14} The code has been extensively validated⁴ with stability, accuracy, and efficiency demonstrated. The code has a multiple zone simulation capability that allows the computational domain to be decomposed and adapted to complex geometries in a straightforward manner. GASP employs finite volume discretization of the integral form of the Navier-Stokes equations as a description of the fluid dynamics. Additional equations can be included for species continuity and turbulence closure.⁴ This version is commonly run employing up to 20 processors which corresponds to the zonal decomposition. The speedup is about a factor of 10 over the case when our large 3-D case is run on a single processor.^{7, 14}

The rationale for this investigation is that the original VertiCOIL nozzle design gave a fairly uniform gain distribution in the lasing zone when helium was employed as diluent.⁶ However, when nitrogen was substituted as the diluent, the gain peaked just downstream of the nozzle throat and dropped off fairly rapidly as it reached the laser cavity.⁶ This gain “peaking” upstream of the laser mirrors can be detrimental to laser performance. Thus peak gain upstream of the mirrors can cause a loss of chemical efficiency and high power densities on the upstream edge of the mirror. Moving the injectors downstream offers the potential to reduce this deleterious effect by producing a gain distribution which is more uniform, achieving a maximum within the mirror region. Such a gain distribution would then distribute the power load more uniformly over the mirror surface avoiding the deleterious effects.

Further, there has been significant experience with Iodine injectors where the flow emanating from the jet was directly opposed to its partner on the opposite side of the nozzle. It was not known what the difference in performance might be if these jets were interleaved (or staggered). Thus we included this possibility in both the VertiCOIL experimental arrangement and the “exact” numerical simulation.

Approach

In order to realistically simulate the injection process, a nozzle mixing configuration similar to that conducted in previous studies was employed. The baseline nozzle that we examined for our nitrogen-diluted series had been used in earlier helium experiments and CFD simulations by Madden.⁴ In this nozzle the iodine injector jets are located quite far upstream (1.1 cm) from the nozzle throat and consist of banks of opposed (top and bottom) sonic orifices. To improve the design we moved the large injectors closer to the nozzle throat, 0.47 cm upstream of the nozzle throat, and conducted a second and third numerical experiment.⁷ In this experiment the large injectors were interleaved rather than opposed. The purpose of the latter was to establish the degree of communication (top and bottom) between the jets.

Two additional computational grids (Case II and Case III) were developed for use in this investigation. Both grids were generated using Gridgen software (Pointwise Corp., Version 13), a structured grid generator for use on a Silicon Graphics workstation. The principal difference between the two grids generated is that, here, the second grid has a slightly larger laser nozzle throat with respect to the first grid (0.453" versus 0.353"). Identical grid generation methods were applied to both grids, see Figure 2. The grid generated by Madden was used in the first of the three computations presented here and his grid generation method was followed here.⁴ It is the baseline case from which our study of nitrogen diluted systems departed.

The flow conditions are given in Table 2. All flow conditions for these simulations for Cases I-III are as indicated in this table, except that the pressure is reduced in Case III from 60 to 45 torr. It should be noted that in the actual lab experiments that when the throat height is increased and pressure decreased that the yield increases due to a lower pooling reaction loss. For the purpose of these numerical computations it was desired to study the effects the geometry change has on the fluid mechanics and mixing phenomena without adding the complexity of the increased yield in trying to understand the numerical results.

Table 2. Flow rates for the numerical experiments.

Experimental Flow Conditions: Simulation 1	
I ₂	0.85 mmol/sec
Cl ₂	40.6 mmol/sec
Utilization	0.98
N ₂ Primary Flow	164 mmol/sec
N ₂ Secondary Flow	40 mmol/sec
Duct Pressure	60 Torr
Duct Temperature	278 K
P _∞ secondary	176.6 Torr
T _∞ secondary	423.2 K
Yield	0.615

When the configuration for Case I is operated as a nitrogen-diluted laser the iodine injector quickly penetrates to the centerline and good utilization of the O₂(¹Δ) within the iodine jet was obtained.⁶ I₂ disappears almost immediately in the subsonic portion of the main flow. The I* concentration builds up inside the high velocity portion of the jet to a very high level and persists down-stream as the jet begins to twist and break up. As a result, the gain builds up and to a very high peak value within the subsonic region of the flow and drops off rapidly as it enters the optical cavity. This occurs because of the slower velocity of the flow in the nitrogen-diluted nozzle than in the helium-diluted nozzle. For this reason we moved the large injectors closer to the nozzle throat, 0.47 cm upstream of the nozzle throat, and conducted a second and third numerical experiment. In these experiments the large injectors were interleaved rather than opposed.

Results

Results from three simulations are reported here: Case I, subsonic injection I₂ with the large injectors located far upstream, 1.1 cm upstream of the geometric throat and a throat height of 0.353"; Case II, subsonic injection of I₂ with the injectors located 0.47 cm upstream of the geometric throat and a throat height of 0.353"; and Case III, subsonic injection of I₂ with the injectors located 0.47 cm upstream of the throat and the nozzle throat enlarged to 0.453".

Case I with the injectors located far upstream (helium diluent baseline^{4,6} nozzle) was run with nitrogen diluent for comparison. We show the penetration by observing the N_2/I_2 stream as it mixes in Figure 3a and 3b. We note that penetration into the main stream is good and reaches the centerline at the nozzle throat. Figures 4a and 4b which provide the I_2 profile show that $O_2(^1\Delta)$ penetration into the jet has resulted in rapid dissociation of the I_2 in the first couple of millimeters of the flow. Figures 5a and 5b show an average gain plot with 2%/cm gains appearing in the subsonic section of the nozzle. Rather obviously, penetration, mixing and reaction are taking place too far upstream of the laser cavity leading to much reduced gains in the cavity. By inference, this is not an efficient lasing situation (which is confirmed by running a Blaze II quasi-2D Fabry-Perot power calculation for this case and by experiment in the laboratory in which the laser efficiency never exceeded 16%^{8,9}).

Our numerical experiment was continued with the re-designed nozzle injectors by moving the Iodine injector further downstream to 0.47 cm upstream of the throat. The calculation was repeated to see how far the gain zone was displaced downstream. Figures 6a-c show the results of the N_2/I_2 study of penetration. Penetration appears to be reasonably complete and Figures 7a and 7b show that I_2 gets as far as the nozzle divergent section before disappearing completely. We see a result of the design change first in the extended passage of unreacted I_2 downstream in Figures 7a and 7b. Penetration of the jets by $O_2(^1\Delta)$ is shown in Figure 8. Here we see that there is about a 50% utilization of $O_2(^1\Delta)$ inside the jets prior to lasing. This represents a fairly complete mixed and reacting flow case. When we look at the gain distributions in Figures 9a and 9b we see that gains exceeding 1.6% occur just upstream of leading edge of the mirror. These gains drop smoothly to 1.1% as they exit the important cavity region. While the increased cavity gain is encouraging with respect to Case I, we note that there is still some room for improvement in our basic design. We also note the highly three dimensional nature of the flowfield in Figure 10 which shows a typical Mach number distribution in this kind of a mixing nozzle.

As a result, we examined Case III, which is identical to Case II as far as location of the I_2/N_2 jets. However we increased the throat height by 28% to 0.453". This lowered the pressure and decreased the penetration into the flow. If one observes the nitrogen traces in the N_2/I_2 jet stream one can immediately see that centerline penetration is not achieved, Fig. 11. Approximately 90% of the flow channel height is filled with the jet within the important laser cavity region, see Figure 11. Figures 12a and 12b for Case III illustrate that the iodine disappearance looks very much like that found in Case II, Figs. 7a and 7b. When one examines the gain plots in Figures 13a and 13b one notes smooth gains curves exceeding 1.25% proceed much of the way through the important cavity region. Thus, from the non-lasing CFD results it is really difficult to tell if case III is an improvement over case II.

Conclusions

In order to determine the relative merits of the three cases studied we compare them with the calculated gain distributions for a helium diluted laser nozzle (analogous flow conditions to that shown in Table 2 were used for this comparison) of the same design as Case I. Figure 14 shows a comparison of the maximum of the average gain of these cases with the helium diluent case because a large number of measurements are available with helium and this helium case should show near optimum performance for this type of nozzle-mixing arrangement. Indeed a smooth gain zone of 1.3% cm^{-1} through the important cavity region is observed for this comparison case. A direct substitution of helium for nitrogen as in Case I of our three new numerical experiments shows that the gain peaks long before reaching the optical cavity to be utilized in the lasing process. Thus, this is the poorest performing laser nozzle for our nitrogen diluent case. The lower velocities and more completed mixing in the predominantly nitrogen stream account for the early peaking of the gain and the lower gain in the cavity region. Case II is nearly identical to Case I, but has injection interleaved and relocated as close to the nozzle throat as was physically possible and still inject upstream of the throat. (Note, we reserve the experiments with injection at the fluid dynamic throat for later comparisons.)

The injection location in Case II forces the gain zone to move downstream so that it fills the lasing zone much better than Case I. This is simply the effect of the delayed injection. Case III is identical to Case II except that the throat height is increased by 28% and the pressure is lower. In this lower pressure case, the temperature is slightly lower and the gain is distributed better throughout the important cavity region. Everything being equal, we would expect best gain performance from Case III. However, due to the larger throat (needed to reduce the pressure) this case underpenetrated by about 10%. So, while we did fill the cavity better we did not quite get the penetration that we desired. It appears that the two effects (better cavity filling and lower penetration) just about compensate for the other.

Our study was not totally conclusive regarding the interleaving of jets versus the opposing geometry. However, it appears that properly penetrated jets do tend to communicate across the centerline.

We have conducted experiments with VertiCOIL hardware configured for Cases I, II and III.⁹ We found that the laser performance was successively improved in each case. The numerical results indicate Case III would likely require increased penetration in order to see any improvement over Case II. We observed about a 15% improvement when this was done in the laboratory. Overall, these findings are consistent with our observations in the laboratory.

Acknowledgments

Portions of this work were supported by the Defense Advanced Research Projects Agency, the National Supercomputing Alliance, and by the Air Force Research Laboratory Small Business Technology Transfer Program.

References

1. Hager, G. D., Watkins, L. J. Meyer, R. K., Johnson, D. E., Bean, L. J., and Loverro, D., "A Supersonic Chemical Oxygen-Iodine Laser" AFWL Technical Report 87-45, Kirtland AFB, NM, (1988).
2. Truesdell, K. A., Lamberson, S. E., and Hager, G. D., "Phillips Laboratory COIL Technology Overview," AIAA 92-3003, AIAA 23rd Plasmadynamics and Lasers Conference, Nashville TN, July, 1992.
3. Buggeln, R. C. and Shamroth, S., Lampson, A. I., and Crowell, P. G., "Three-Dimensional (3-D) Navier-Stokes Analysis of the Mixingna Power Extraction in a Supersonic Chemical Oxygen Iodine Laser (COIL) with Transverse I₂ Injection," AIAA 94-2435, 25th AIAA Plasmadynamics and Lasers Conference, June 20-23, 1994, Colorado Springs, Co.
4. Madden, T. J. and Solomon W. C. " A Detailed Comparison of a Computational Fluid Dynamic Simulation and a Laboratory Experiment for COIL Laser," AIAA 97-2387, 28th AIAA Plasmadynamics and Lasers Conference, Atlanta, GA, June, 1997.
5. Masuda, W., Hishida, M., Hirooka, S., Azami, N. and Yamada, H., "Three Dimensional Mixing/Reacting Zone Structure in a Supersonic Flow Chemical Oxygen-Iodine," JSME International Journal Series B-Fluids and Thermal Engineering, **41**, No. 2, pp. 209-215 (1997).
6. Fockler, L. A., "Large Scale Simulations of Chemical Oxygen Iodine Laser Flow Fields Using Nitrogen Diluent", M.S. Thesis, Mechanical Engineering, University of Illinois at Urbana-Champaign, 1999.
7. Stromberg, D. S., "Computational Fluid Dynamic Analysis of a Chemical Oxygen Iodine Laser using Nitrogen Diluent", M.S. Thesis, Aeronautical and Astronautical Engineering, University of Illinois at Urbana-Champaign, 2000.
8. Rittenhouse, T.L., Phipps, S.P., and Helms, C.A., "Performance of a 5 cm gain length supersonic Chemical Oxygen-Iodine Laser", IEEE J. Quantum Electronics, **35**, pp. 857-865 (1999).
9. Carroll, D. L., King D. M., Fockler L., Solomon W. C., Sentman, L. H., and Fisher C. H., "High-Performance Chemical Oxygen-Iodine Laser Using Nitrogen Diluent for Commercial Applications", IEEE J. Quantum Electronics, **36**, pp. 40-51 (2000).
10. Carroll, D. L., "Modeling High Pressure Chemical Oxygen-Iodine Lasers," AIAA Journal, **33**, No. 8, pp. 1454-1462 (1995).
11. Carroll, D. L., "Optimizing High Pressure Chemical Oxygen-Iodine Lasers," Proc. of the International Conf. On Lasers '95, Society of Optical and Quantum Electronics, McLean, VA (1996).
12. Heaven, M.C., "Studies of Energy Transfer Processes of Relevance to Chemically and Optically Pumped Lasers," Emory University AFOSR/NR F49620-92-J-0073 (1994).
13. Fuller, E. J., and Walters, R.W. "Navier-Stokes Calculations for 3-D Gaseous Fuel Injection with Data Comparisons," AIAA Paper No. 91-5072, Dec 1991.
14. Vitt, P. H., Riggins, D. W. and McClinton, C., R., "The Validation and Application to Supersonic Mixing and Reaction Flows" AIAA Paper No. 93-0606, 31st Aerospace Sciences Meeting, January 1993.

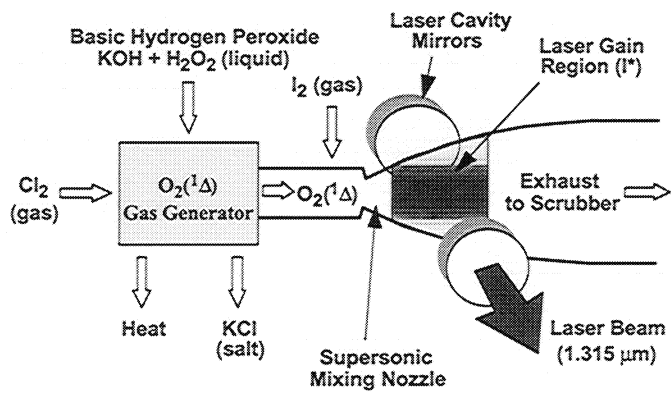


Figure 1. Schematic of a typical COIL device.

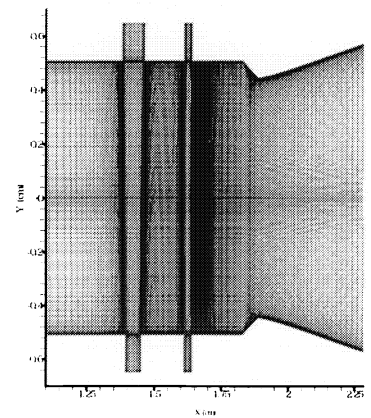
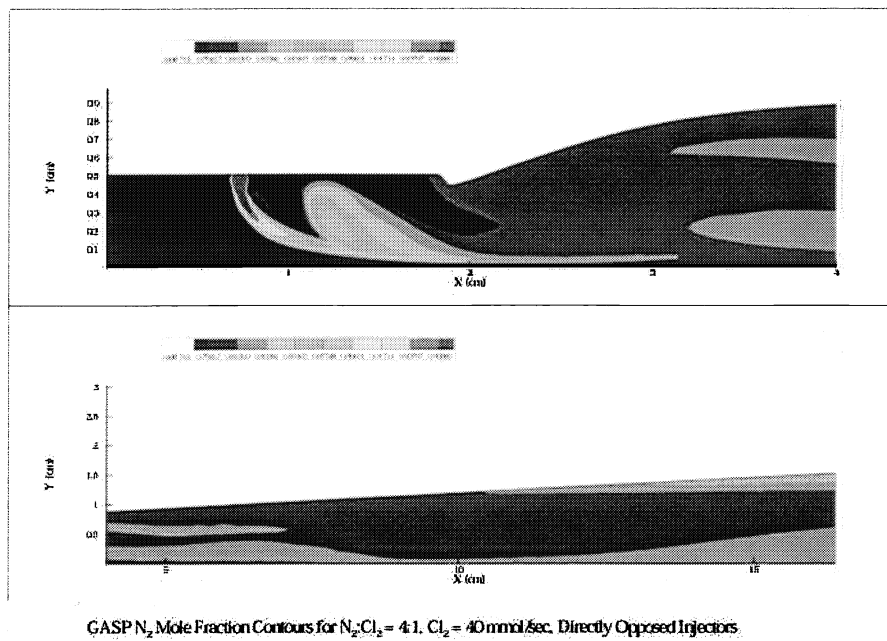
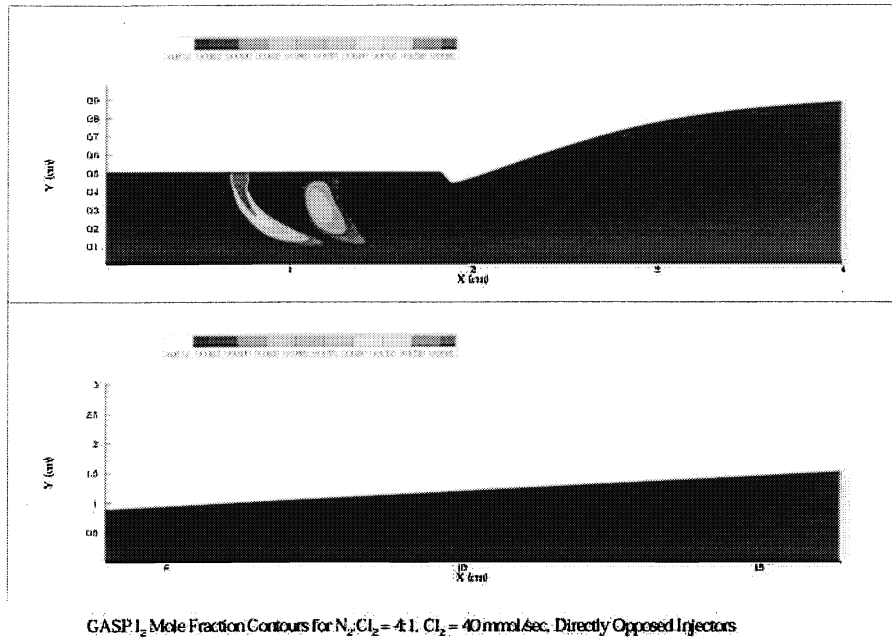


Figure 2. CFD grid in the injector-throat region.

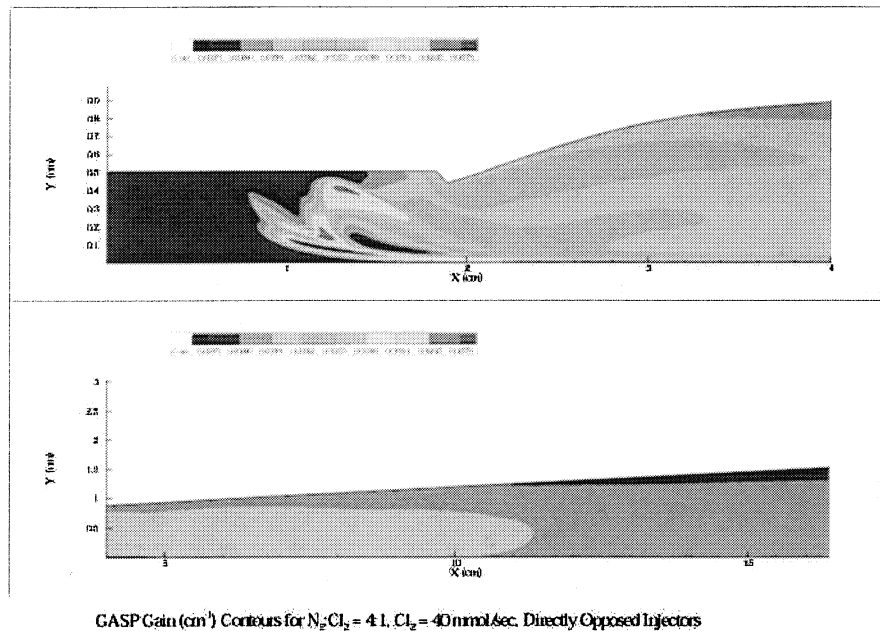


GASP N_2 Mole Fraction Contours for $N_2/Cl_2 = 4:1$, $Cl_2 = 40$ mmol/sec. Directly Opposed Injectors.

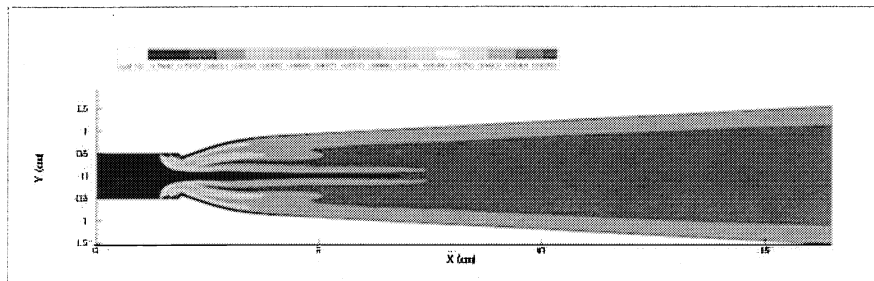
Figures 3a and 3b. GASP N_2 mole fraction contours for $N_2/Cl_2 = 4:1$, $Cl_2 = 40$ mmol/sec. Directly opposed injectors.



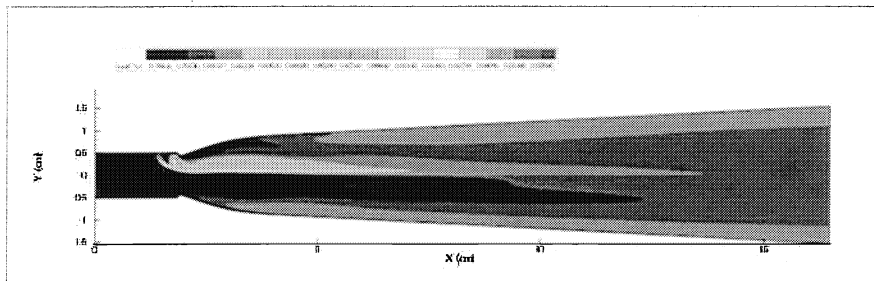
Figures 4a and 4b. GASP I_2 mole fraction contours for $N_2/Cl_2 = 4:1$, $Cl_2 = 40$ mmol/sec. Directly opposed injectors.



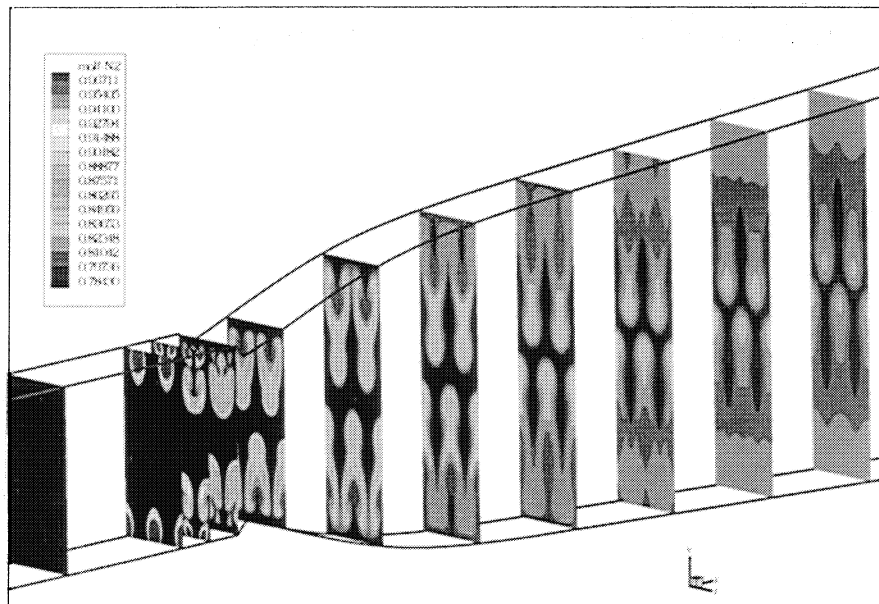
Figures 5a and 5b. GASP gain ($1/cm$) contours for $N_2/Cl_2 = 4:1$, $Cl_2 = 40$ mmol/sec. Directly opposed injectors.



(a): GASP N_2 Mole Fraction Contours for Simulation 1 (Throat Height = 0.353") - Center of Small Injector

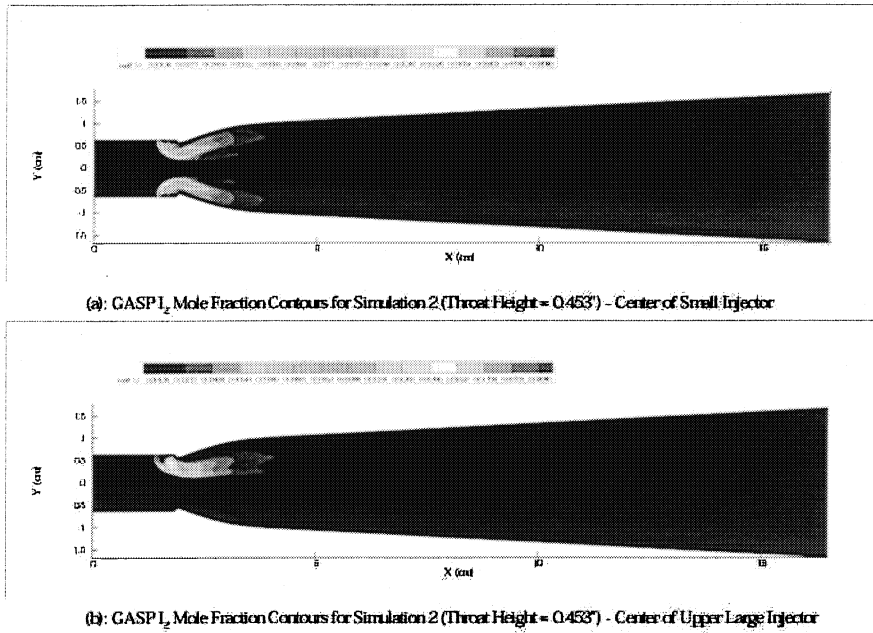


(b): GASP N_2 Mole Fraction Contours for Simulation 1 (Throat Height = 0.353") - Center of Upper Large Injector



(c): GASP N_2 Mole Fraction Contours for Simulation 1 (Throat Height = 0.353")

Figures 6a-c. GASP N_2 mole fraction contours for $N_2/Cl_2 = 4:1$, $Cl_2 = 40$ mmol/sec. Throat height of 0.353". Interleaved injectors.



Figures 7a and 7b. GASP I_2 mole fraction contours for $N_2/Cl_2 = 4:1$, $Cl_2 = 40$ mmol/sec. Throat height of 0.353". Interleaved injectors.

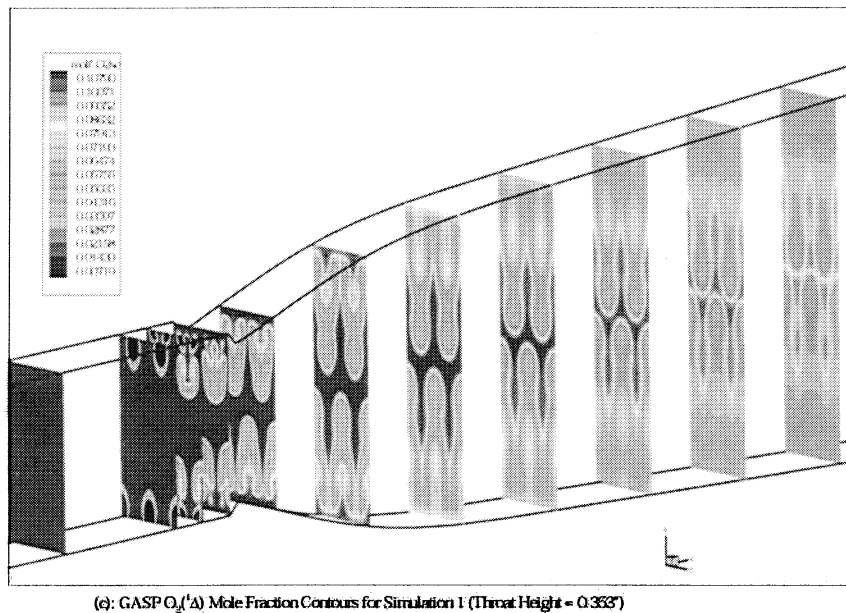
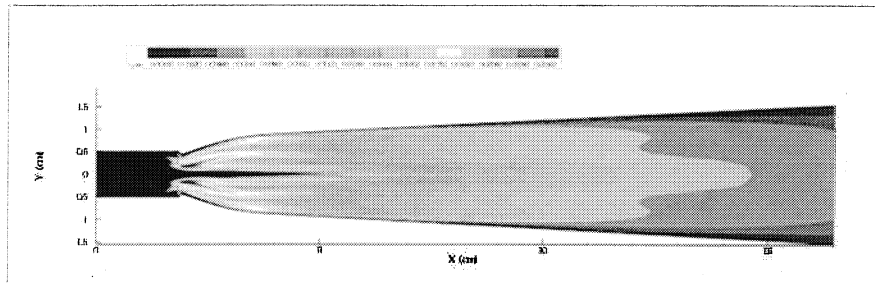
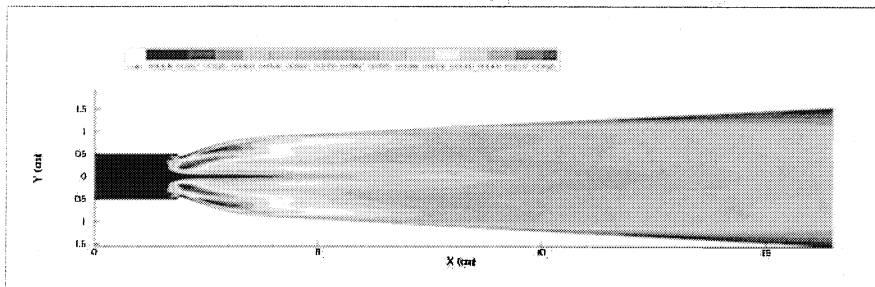


Figure 8. GASP $O_2(1\Delta)$ mole fraction contours for $N_2/Cl_2 = 4:1$, $Cl_2 = 40$ mmol/sec. Throat height of 0.353". Interleaved injectors.

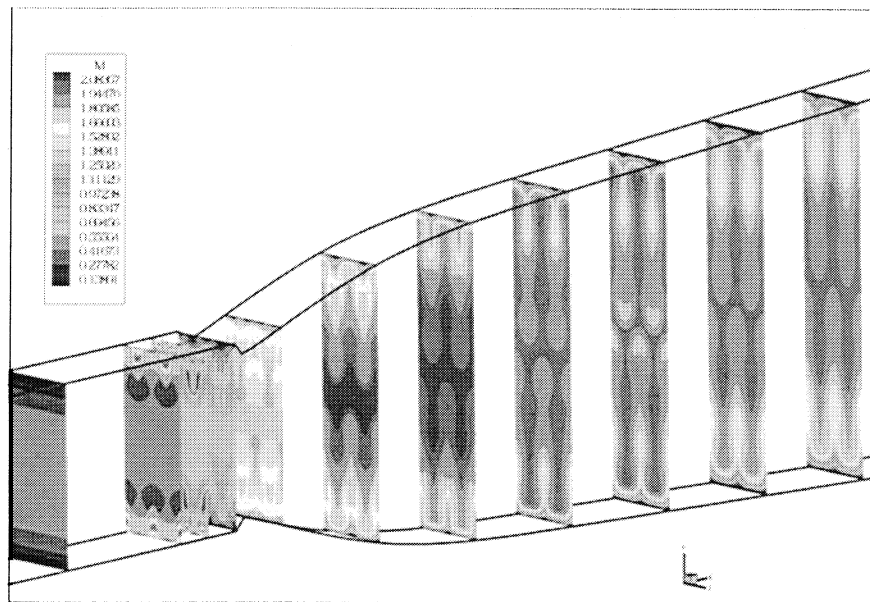


(a): GASP Gain (cm^{-1}) Contours for Simulation 1 (Throat Height = 0.353") - Center of Small Injector



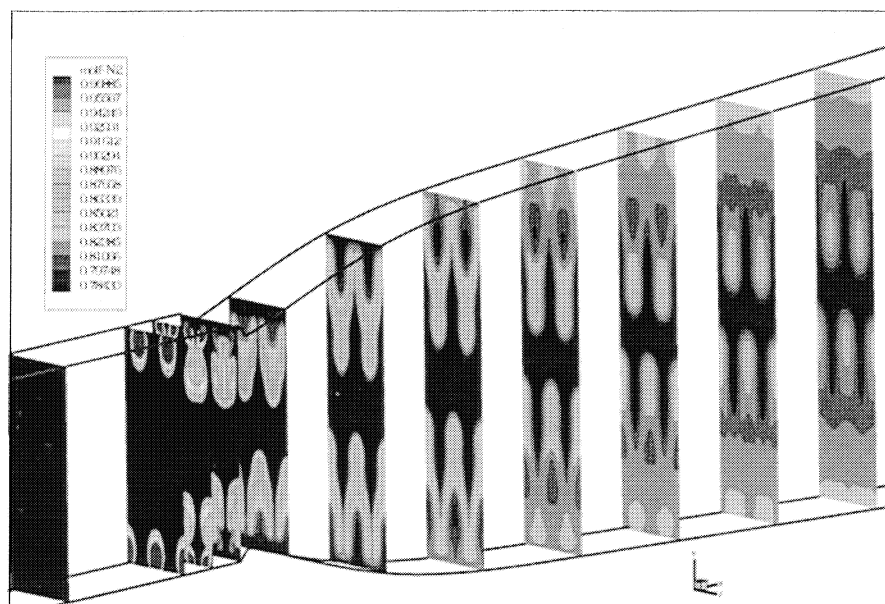
(b): GASP Average Gain (cm^{-1}) Contours for Simulation 1 (Throat Height = 0.353")

Figures 9a and 9b. GASP gain ($1/\text{cm}$) contours for $\text{N}_2/\text{Cl}_2 = 4:1$, $\text{Cl}_2 = 40$ mmol/sec. Throat height of 0.353". Interleaved injectors.



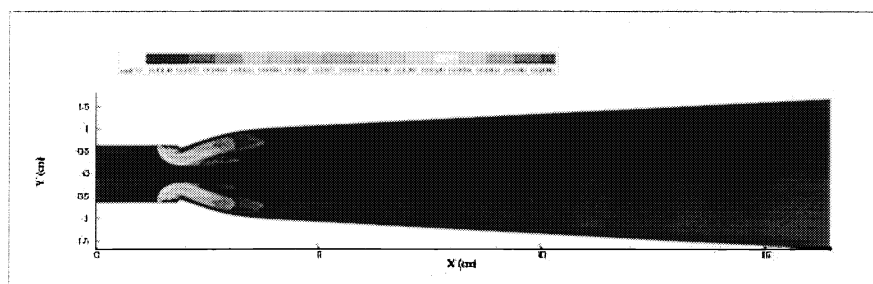
(c): GASP Mach Number Contours for Simulation 1 (Throat Height = 0.353")

Figure 10. GASP Mach number contours for $\text{N}_2/\text{Cl}_2 = 4:1$, $\text{Cl}_2 = 40$ mmol/sec. Throat height of 0.353". Interleaved injectors.

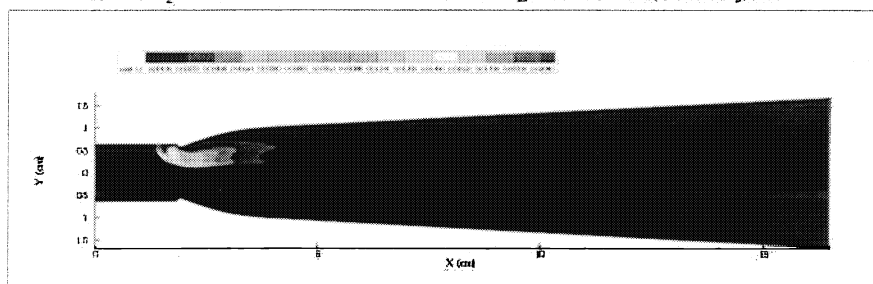


(c) GASP N_2 Mole Fraction Contours for Simulation 2 (Throat Height = 0.453")

Figure 11. GASP N_2 mole fraction contours for $N_2/Cl_2 = 4:1$, $Cl_2 = 40$ mmol/sec. Throat height of 0.453". Interleaved injectors.

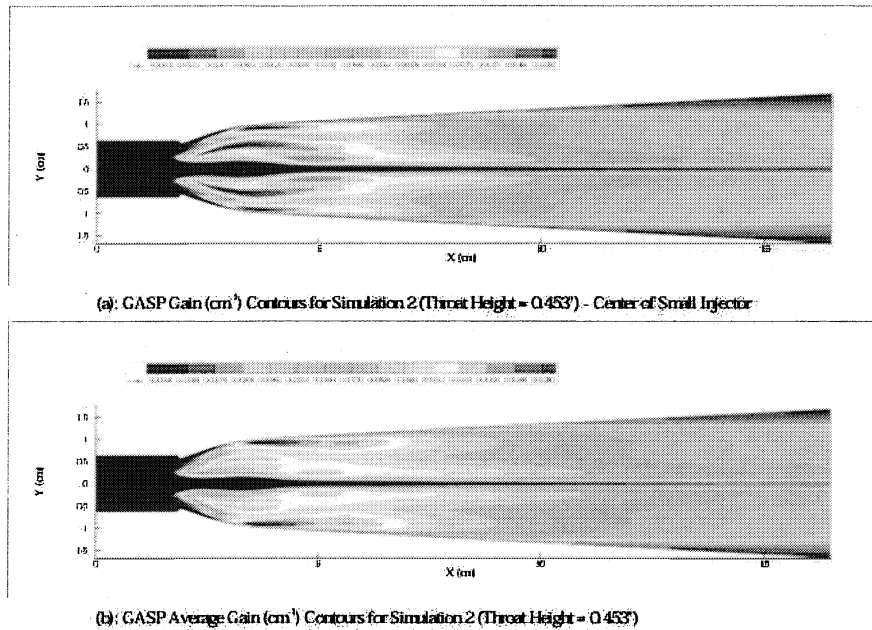


(a) GASP I_2 Mole Fraction Contours for Simulation 2 (Throat Height = 0.453") - Center of Small Injector



(b) GASP I_2 Mole Fraction Contours for Simulation 2 (Throat Height = 0.453") - Center of Upper Large Injector

Figures 12a and 12b. GASP I_2 mole fraction contours for $N_2/Cl_2 = 4:1$, $Cl_2 = 40$ mmol/sec. Throat height of 0.453". Interleaved injectors.



Figures 13a and 13b. GASP gain ($1/\text{cm}$) contours for $\text{N}_2/\text{Cl}_2 = 4:1$, $\text{Cl}_2 = 40 \text{ mmol/sec}$. Throat height of 0.453". Interleaved injectors.

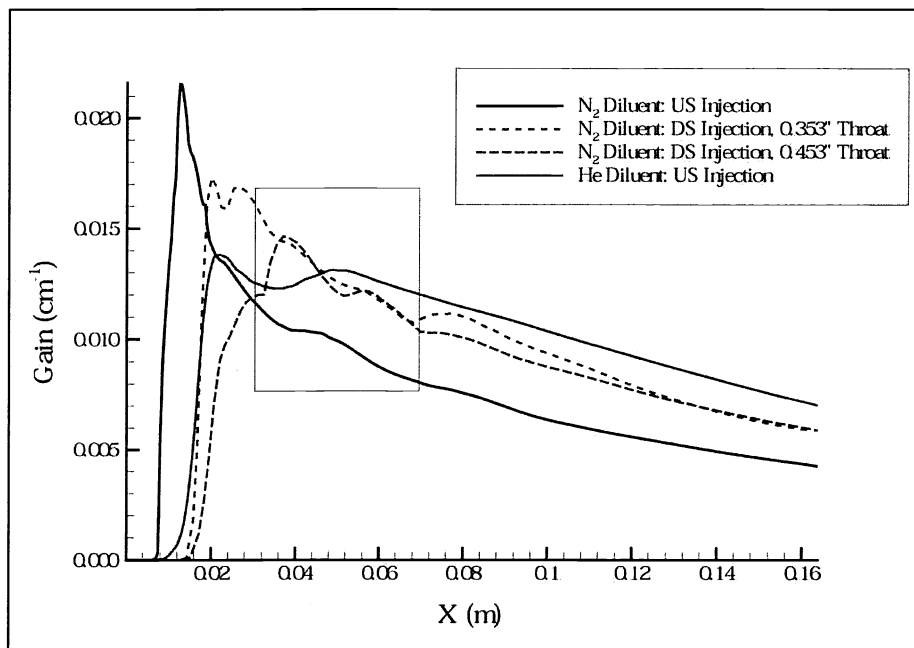


Figure 14. Comparison of the maximum average gain as a function of distance in the flow direction. In all cases, the throat is located at approximately 0.02 m. US denotes I_2 injection 1.1 cm "upstream" of the throat, DS denotes injection further "downstream" at 0.47 cm upstream of the throat.